

Optical excitations of Peierls-Mott insulators with bond disorder

J Rissler[†], F Gebhard[†] and E Jeckelmann[‡]

[†] Fachbereich Physik, Philipps-Universität Marburg, D-35032 Marburg, Germany

[‡] Institut für Physik, KOMET 337, Johannes Gutenberg-Universität, D-55099 Mainz, Germany

E-mail: rissler@staff.uni-marburg.de

Abstract. The density-matrix renormalization group (DMRG) is employed to calculate optical properties of the half-filled Hubbard model with nearest-neighbor interactions. In order to model the optical excitations of oligoenes, a Peierls dimerization is included whose strength for the single bonds may fluctuate. Systems with up to 100 electrons are investigated, their wave functions are analyzed, and relevant length-scales for the low-lying optical excitations are identified. The presented approach provides a concise picture for the size dependence of the optical absorption in oligoenes.

Submitted to: *JPCM*

PACS numbers: 71.10.Fd, 71.20.Rv, 71.35.Cc, 78.66.Qn

1. Introduction

One of the main goals in the field of π -conjugated polymers is the fabrication of opto-electronic devices such as solar cells, light-emitting diodes, and displays [1]. The operating part of these devices is a thin (spun-cast) film of a polymer between two electrical contacts through which holes and electrons are injected into the film. Evidently, the resulting excited electron-hole states in the disordered polymer film determine the optical properties of the whole device. The simplest access to them is the measurement of the absorption of the polymer film.

More information is provided by the so-called oligomer approach [2]. Oligomers of increasing length ℓ are synthesized where ℓ is a multiple of a monomer repetition unit. Quite universally, one observes a bathochromic shift for the lowest-energy absorption peak, i.e., $E_{\text{ex}}(\ell)$ monotonically decreases as a function of ℓ . For medium-sized oligomers there is a regime where $E_{\text{ex}}(\ell)$ drops almost linearly in $1/\ell$, and only the smallest oligomers may deviate from the linear fit. For larger oligomers, however, $E_{\text{ex}}(\ell)$ appears to saturate quickly [3]. It is also known, that perfectly-ordered polymers still have a finite gap for optical excitations, i.e., they are insulators [4].

The aim of this work is to study this length dependence of the optical absorption theoretically and identify the existing length scales in ordered and disordered oligomers. As a generic example for a π -conjugated system one can choose polyacetylene and the homologous oligomers, the oligoenes. Here, ℓ is given by the number L of carbon atoms in the conjugated system whose average distance is a_0 , $\ell = (L - 1)a_0$.

As a starting point, ordered oligoenes can be described by the Peierls model [5] which correctly describes polymers as insulators. Moreover, in a Peierls insulator the lowest excitation energy at the Fermi vector k_F (antiperiodic boundary conditions) becomes

$$E_{\text{ex}}^P(L) = \epsilon_+^P(k_F) - \epsilon_-^P(k_F) = 2t\Delta + \frac{t\pi^2(4 - \Delta^2)}{\Delta} \frac{1}{L^2} \quad (1)$$

for large systems, $L \gg \pi\sqrt{-1 + 4/\Delta^2}$. The parameter Δ accounts for the bond alternation. From (1) one can conclude that the convergence towards the Peierls gap is quadratic in $1/L$. This result does not contradict the experimental observation of a linear behavior in $1/L$ for medium-sized oligomers, as in this range a Taylor expansion is always a good approximation.

Apart from the length scales set by the nominal oligomer size L there is another important length scale in the problem due to the electron-electron interaction. The importance of the electron-electron interaction has been pointed out a long time ago [6, 7]. In fact, well-ordered polydiacetylenes display excitons with a substantial binding energy [4]. Calculations for ordered oligomers and polymers have been performed recently on the basis of Wannier theory [8], the GW approximation to Density Functional Theory [9, 10], strong-coupling approaches [11, 12], and numerical investigations of interacting electron systems [13, 14, 15, 16] and interacting electron-phonon systems [17]. These investigations show that the average electron-hole distance,

$\langle r_{\text{eh}} \rangle$, is an important length scale for the optical absorption of oligomers, specific to the monomer building unit. This explains the deviations for the smallest oligomers from an expected behavior, as finite-size effects seriously hamper the formation of a bound electron-hole pair.

The microscopic theoretical approaches presented so far apply to ordered chains. Disorder may break down longer oligomers into shorter, ordered chains. According to a basic statistical analysis of this ‘hard disorder’ model [18], oligomers with the full nominal length L are highly unlikely to be found for large L , and the ‘typical’ chain length, L_{typ} , increases only very slowly with L . This is one reason of the observed saturation effect of E_{ex} . ‘Soft disorder’ is induced by a random bending of ordered segments against each other. The electron-transfer matrix elements between the segments then depend on the (small) bending angle ϑ . As shown in Ref. [19], this can turn the quadratic dependence (1) back to a linear behavior of $E_{\text{ex}}(L)$ on $1/L$,

$$E_{\text{ex}}^{\text{sp}}(L) = 2t\Delta + b'/L. \quad (2)$$

This also supports the observation of a linear $1/L$ behavior of $E_{\text{ex}}(L)$ for medium-sized oligomers. L_{typ} is in this case defined as the correlation length for the coplanarity of ordered segments.

In general, the length dependence of the optical excitations of a polymer film is an interplay between three different length scales: L , the nominal length of the oligomers, which are broken down into segments of typical length L_{typ} by disorder effects, and r_{eh} , defined by the electron-electron interaction. A minimal microscopic description of oligoenes should combine the microscopic approaches for the ordered systems with the statistical ones for the disordered systems in order to cover all three length scales. Therefore, a suitable Hamiltonian includes a bond alternation due to the Peierls distortion, possible formation of bound electron-hole pairs due to the Coulomb interaction, and soft disorder due to torsion or bending of the oligomer chain. The experimental situation where long oligomers appear to be cut into smaller chains can be taken into account by a suitable average over chain-length distributions. A more quantitative analysis will also consider polaronic effects due to the electron-lattice coupling.

This program is carried out in the following to some extent. In Sect. 2 the extended Peierls-Hubbard model is defined which takes into account the bond alternation as well as a local and nearest-neighbor Coulomb interaction in perfectly ordered chains. In Sect. 3 some details are given on the density-matrix renormalization group (DMRG) [20] which is used for the numerical investigation of this model, and a scheme is recalled to analyze excited-state wave functions in interacting electron systems [21]; this scheme proves equally applicable in the presence of disorder. In Sect. 4 results are presented for ordered chains. For the single-particle gap and the resonance of the first excited state a quadratic convergence in $1/L$ is found, and plausible explanations are given for this observation. In Sect. 5 the soft disorder in the chain is modeled by electron-transfer amplitudes for the single bonds which depend on randomly chosen torsion angles. The

consequences of soft disorder on the excitation energies are investigated as well as the wave functions for chains of fixed size, and hard disorder is simulated by a simple profile for the distribution of chain lengths. Sect. 6 summarizes the main results.

2. Model Hamiltonian

This work focuses on the general properties of π -conjugated oligomers. A generic model is the extended Peierls-Hubbard (EPH) model for oligoenes which provides a good compromise between the accuracy of the description and a reasonable yet tractable system size.

2.1. Extended Peierls-Hubbard model

One starts from a minimal basis of orthogonal p_z -(Wannier-)orbitals $\phi_i(\vec{x})$ centered at the i th site (carbon atom) of the oligomer chain at \vec{r}_i . The operators $\hat{c}_{i,\sigma}^\dagger$ ($\hat{c}_{i,\sigma}$) create (annihilate) an electron with spin σ in the orbital $\phi_i(\vec{x})$. The number operator $\hat{n}_{i,\sigma} = \hat{c}_{i,\sigma}^\dagger \hat{c}_{i,\sigma}$ counts the electrons with spin σ on site i , and $\hat{n}_i = \hat{n}_{i,\uparrow} + \hat{n}_{i,\downarrow}$. The EPH Hamiltonian reads

$$\begin{aligned} \hat{H}_{\text{EPH}} = & (-t) \sum_{i=1,\sigma}^{L-1} \left(1 - (-1)^i \frac{\Delta}{2} \right) (\hat{c}_{i+1,\sigma}^\dagger \hat{c}_{i,\sigma} + \text{h.c.}) + U \sum_{i=1}^L \left(\hat{n}_{i,\uparrow} - \frac{1}{2} \right) \left(\hat{n}_{i,\downarrow} - \frac{1}{2} \right) \\ & + V \sum_{i=1}^{L-1} (\hat{n}_i - 1) (\hat{n}_{i+1} - 1) . \end{aligned} \quad (3)$$

Open boundary conditions apply. The first term represents the kinetic energy of the electrons and their potential energy with respect to the atomic cores. The electron-transfer integral t is supposed to be finite only between nearest neighbors. The geometric effect of alternating single and double bonds is accounted for through the variation of t by the amount of Δ . In this form the model allows the investigation of properties of perfectly ordered chains. The geometric relaxation of the excited state, however, is neglected.

The next two terms in (3) describe the electron-electron interaction. The occupation of a single site with two electrons costs the Coulomb energy U (Hubbard interaction). Two electrons on two neighboring sites repel each other with strength V . A chemical potential is added in such a way that half filling, one electron per orbital, is guaranteed due to particle-hole symmetry.

Natural units are used in which $a_0 = t = e = \hbar = 1$. This leaves three parameters for the description of real materials: U , V and Δ . For the presented calculations later on three parameter sets from the literature are studied, which have been designed to describe polyacetylene.

The first two parameter sets (**A**, **B**) lead to bound electron-hole pairs for the lowest excited state but the third one, **C**, does not. The parameter sets allow to test the analysis presented in Sect. 3.2, therefore, also parameter set **C** is included which does not reflect the experimental reality.

Table 1. Three parameter sets used in equation (3).

Label	Reference	$\Delta(t)$	$U(t)$	$V(t)$
A	[12]	0.38	3	1
B	[13]	0.2	3	1.2
C	[14]	0.11	2.5	0.625

3. Methods

3.1. Density-Matrix Renormalization Group (DMRG)

The DMRG [20] is used to obtain the ground state and excited states of the EPH Hamiltonian (3) in a numerically exact way. This variational method is very accurate for quasi one-dimensional systems with hundreds of electrons; see [22] for a review. In this work the maximum number of block states kept to describe the target states is $m = 400$. During a calculation m is increased stepwise and for each m a converged state is determined. From an extrapolation of the discarded weight and the target-state energy, the DMRG error in the energies has been calculated. This error is $\eta_s \leq O(10^{-6})$ for the energies of single target states, e.g., for $E_{\text{ex}}(L)$. The calculation of the optical spectra involves up to ten target states. The increase in target states also increases the DMRG error to $\eta_a \leq O(10^{-3})$. The DMRG error is of the same order as the resulting energy distributions due to the disorder only for very long chains and very small disorder; the DMRG error is much smaller in all other cases.

The total spectral weight W_{tot} , i.e., the frequency integral over the optical conductivity $\sigma(\omega)$, can be expressed in terms of the ground-state expectation value of the kinetic-energy operator [23],

$$W_{\text{tot}} = \int_{-\infty}^{\infty} \sigma(\omega) d\omega = -\frac{\pi}{2L} \langle \hat{T} \rangle . \quad (4)$$

Consequently, the contribution $W_s(L)$ of a certain state at the resonance energy E_s is given by

$$W_s(L) = \frac{\alpha(E_s)}{W_{\text{tot}}} \quad (5)$$

$$\alpha(E_s) = \frac{\pi}{L} \left| \langle \Phi_s | \hat{D} | \Phi_0 \rangle \right|^2 \quad (6)$$

where $\hat{D} = \sum_l l(\hat{n}_l - 1)$ is the current operator and $|\Phi_0\rangle$, $|\Phi_s\rangle$ are the ground state and s th excited state, respectively.

The maximum length L of the investigated oligomers is varied in the range $8 \leq L \leq 200$. For the calculation of $E_{\text{ex}}(L)$ systems of size $L = 8, 12, 16, 18, 20, 24, 28, 40, 56, 76, 100, 140, 200$ are studied. For spectra and disordered oligomers, only the system sizes $L = 12, 16, 20, 24, 28, 56, 76, 100$ are considered. The results for $L = 4$, especially for the disordered cases, indicate that the influence of the boundaries is dominant. Therefore, $L = 4$ is not included here.

3.2. Analysis of wave functions

In a recent publication [21] two of the authors formulated a general interpretation scheme for excited-state wave functions in correlated electron systems. Here, it is adapted to wave functions as obtained from the EPH.

The scheme is based on the description of the absorption process with Fermi's golden rule or the Kubo formula. There, the oscillator strength $f_{s,0}$ for the optical transition from the ground state $|\Phi_0\rangle$ to some excited state $|\Phi_s\rangle$ ($s = 1, 2, \dots$) is proportional to the square of the absorption amplitudes $A_{s,0}$. With this quantity one can define a coarse-grained, spin-averaged electron-hole density $p_{s,0}(i, j)$ for electrons in an atomic volume V_i and holes in an atomic volume V_j .

In the case of the EPH wave functions, one has to replace the general orbitals $\varphi_p(\vec{x})$ in the description by the Wannier orbitals $\phi_i(\vec{x})$ used in the motivation of (3). The fact that the overlap between Wannier orbitals is negligible simplifies $p_{s,0}(i, j)$ and one finds

$$p_{s,0}(i, j) = \sum_{\sigma} \left| \langle \Phi_s | \hat{c}_{j,\sigma}^{\dagger} \hat{c}_{i,\sigma} | \Phi_0 \rangle \right|^2 \quad (7)$$

Finally, after normalization, one can *interpret*

$$P_{s,0}(i, j) = \frac{p_{s,0}(i, j)}{\sum_{i,j} p_{s,0}(i, j)} \quad (8)$$

as the probability to find an electron-hole pair with the atomic coordinates (i, j) in the excited state with respect to the ground state. That means that one can only measure an excitation, if the respective excited state has an electron-hole character with respect to the ground state.

With the help of the probability distribution $P_{s,0}(i, j)$ one can derive various averages. For example, one may approximate the oligoene structure by a perfectly linear chain with a constant lattice spacing. Then, $r_{\text{eh}} = |i - j|$ is the distance between two carbon atoms i, j , and the probability to find an electron-hole pair at a distance r_{eh} is given by

$$\overline{P}_{s,0}(r_{\text{eh}}) = \sum_{i,j} P_{s,0}(i, j) \delta_{r_{\text{eh}}, |i-j|} . \quad (9)$$

The average electron-hole distance is then given by

$$\langle r_{\text{eh}} \rangle_{s,0} = \sum_{r_{\text{eh}}} r_{\text{eh}} \overline{P}_{s,0}(r_{\text{eh}}) . \quad (10)$$

Equations (8), (9) and (10) are used later to interpret the wave functions of the excited states. Apart from figure 5 only the first excited singlet state, the ' 1B_u state', is investigated. Consequently, for $s = 1$ the indices $(s, 0)$ are dropped. Note that the basic equations (8) and (9) can be derived using only one approximation, namely the negligible overlap between Wannier orbitals.

4. Results for ordered chains

4.1. Excitation-energies and electron-hole distances

Figure 1 shows the energies and weights of the first nine optically-allowed excitations for $L = 100$. The DMRG code used here does not distinguish between different symmetry sectors other than total z -component of the spin, total number of particles and particle-hole symmetry of the EPH in (3). Since neither reflection nor inversion symmetry has been incorporated, optically allowed ' B_u ' states alternate with symmetry-forbidden ' A_g ' states of zero weight.

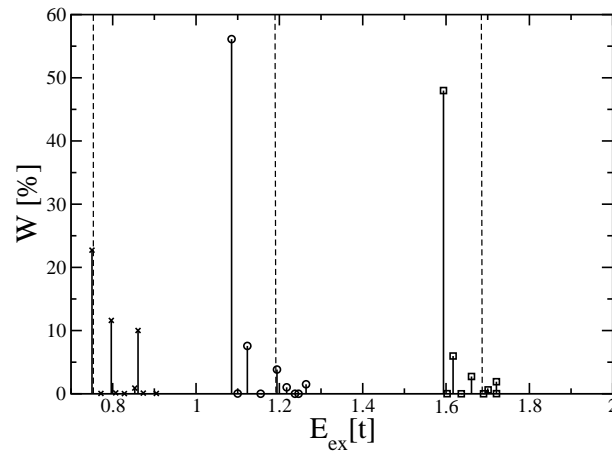


Figure 1. Excitation energies E_{ex} of the first nine optically excited states for $L = 100$. Parameter sets from table 1 **A**, **B**, and **C** are shown from right to left. The weights $W_s(L)$ are obtained from (5). A thin, dashed line marks the one-particle gap (11).

The three different parameter sets lead to optical absorption in different energy regions. For the sets **A** and **B** 60%-70% of the total spectral weight W_{tot} are contained in the first nine states. As expected, the first excited state dominates, $W_1 \approx 50\% W_{\text{tot}}$. In contrast, the first optically allowed excitation no longer dominates the absorption spectrum for the parameter set **C**. Moreover, the first nine optically excited states capture only 45% of the total weight. The missing spectral weight for all parameter sets is presumably distributed among a large number of high-energy states with vanishingly small weights. In the thermodynamic limit, these states eventually merge into an absorption band.

Also shown in figure 1 are the respective values of the one-particle gap, defined by

$$E_{\text{gap}}(L) = E_0(L, N + 1) + E_0(L, N - 1) - 2E_0(L, N). \quad (11)$$

$E_0(L, N)$ is the ground-state energy of an oligoene with N electrons and length L ; for half filling $N = L$. $E_{\text{gap}}(L)$ is the energy needed to create independently an electron and a hole in an oligomer and is therefore a measure for the excitation energy of an unbound electron-hole pair. Consequently, the binding energy of a bound electron-hole

pair is given by

$$E_b(L) = E_{\text{gap}}(L) - E_{\text{ex}}(L) . \quad (12)$$

For $L = 100$, as seen in figure 1, bound electron-hole pairs are present for the parameter sets **A** and **B**, but the binding energy is very small for the parameter set **C**.

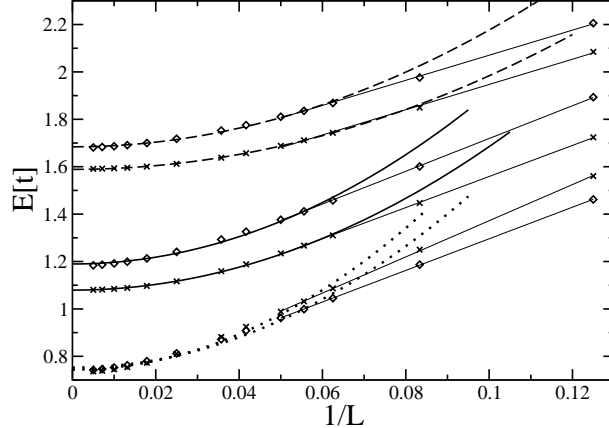


Figure 2. Excitation energy $E_{\text{ex}}(L)$ (crosses) and one-particle gap $E_{\text{gap}}(L)$ (diamonds) for oligoenes with $8 \leq L \leq 200$ carbon atoms from the EPH (3) using the parameter sets of table 1. From top to bottom: Dashed (**A**), solid (**B**), and dotted lines (**C**) are parabolic fits through the data points excluding $L = 8, 12$. Thin lines represent linear fits through the data points for $8 \leq L \leq 24$.

In figure 2 the excitation energy is plotted for the lowest excited state versus the inverse system size in the range $8 \leq L \leq 200$ together with the respective values of the one-particle gap. The parameter sets **A**, **B** result in a bound electron-hole pair in the polymer limit, $E_b > 0$ for all L , whereas the parameter set **C** gives rise to unbound electron-hole pairs, $E_b(L) \rightarrow 0$ for $L \rightarrow \infty$. This is in line with the results of the corresponding work [12, 13, 14]. More important is the *quadratic* convergence of the excitation energy and the single-particle gap with the inverse system size,

$$E_{\text{ex}}^{\text{EPH}}(L) = E_{\infty} + \frac{A}{L^2} . \quad (13)$$

This form very well represents all data points for $16 \leq L \leq 200$, as shown in figure 2. The respective stability indices are $R^2 \geq 0.96$. A linear fit works for small oligoenes, $L \leq 24$, for the reasons discussed in the introduction. This is indicated by thin lines in figure 2. Apparently, such a linear behavior for small oligomers has little to do with the true scaling form of the energy of the bound electron-hole pair.

Table 2 gives the binding energy for $L = 200$, and the curvature A in (13). The quadratic scaling form (13) for a bound electron-hole pair is readily understood in terms of a quasi-particle moving freely in a box of size L . Above the primary excitation energy E_{∞} , the bound electron-hole pair naturally obeys a quadratic dispersion relation,

$$\epsilon_{\text{qp}}(k) = \frac{k^2}{2m_{\text{qp}}} , \quad (14)$$

Table 2. Binding energy E_b , as defined in (12), for the $L = 200$ oligomer (error $\eta_s \leq O(10^{-6})$), curvature A of the quadratic fit (13) for $16 \leq L \leq 200$ in figure 2, and mass of the bound electron-hole pair m_{qp} from (15). The fourth column expresses m_{qp} in units of the electron mass m_e under the assumption $t = 2$ eV and $a_0 = 1.4$ Å. In the last column $\langle r_{eh} \rangle$ from (10) is given as the average electron-hole distance of the $L = 100$ oligomer in units of the lattice constant a_0 .

Label	Reference	E_b	A	m_{qp}	m_{qp}/m_e	$\langle r_{eh} \rangle$
A	[12]	0.090	39.5	0.124	0.24	5.1
B	[13]	0.103	60.6	0.081	0.16	5.9
C	[14]	0.005	93.3	0.053	0.10	17.6

for small $k = n\pi/L$, $1 \leq n \ll L$. In this equation, k denotes only the inverse system size and not the momentum of the particle in an infinite or periodic system. Therefore, one can identify

$$m_{qp} = \frac{\pi^2}{2A} \quad (15)$$

as the mass of the quasi-particle. This quantity is also given in table 2, both in the applied units and in units of the electron mass m_e for $t = 2$ eV and $a_0 = 1.4$ Å. The electron-hole pairs have the expected mass which is somewhat below their reduced mass $\mu = m_e/2$.

It is seen that for both the bound and the unbound cases the excitation energy converges quadratically as a function of $1/L$ as does the single-particle gap. This implies that quasi-particle excitations display a quadratic dispersion near the single-particle gap. This can be verified explicitly for Peierls insulators, see (1), and also for Mott-Hubbard insulators [24, 25]. A quadratic dispersion relation is equivalent to the statement that the group velocity for the single-particle excitations vanishes, and the quasi-particle states at the gap correspond to standing waves. Indeed, the gap formation in Peierls and Mott-Hubbard insulators can be understood as a consequence of the scattering of waves. This picture quite naturally applies to Peierls-Mott insulators, too, so that the gap formation goes hand in hand with a vanishing group velocity for elementary excitations. This is what is found numerically [14, 15, 17], as seen in figure 2. For a more rigorous treatment of gapped systems with few elementary excitations, see [26].

More insight into the properties of the excited states is gained by an analysis of the average electron-hole distance $\langle r_{eh} \rangle$ from (10). In figure 3 one sees that the parameter sets of **A** and **B** lead to a saturation of the electron-hole distance for $L > 50$. The value for $L = 100$ is given in table 2. In other words, $\langle r_{eh} \rangle(L = 100) \ll L$ so that the value at $L = 100$ represents the electron-hole distance in the polymer limit. For the parameter set **C**, $\langle r_{eh} \rangle$ does not appear to saturate which is in accord with a vanishing binding energy, $E_b(L) \rightarrow 0$ for $L \rightarrow \infty$. Apparently, the electron-hole distance is a very important length scale for oligomers.

For the two bound cases, the binding energies E_b are similar and relate to similar values of $\langle r_{eh} \rangle$ in table 2. Comparing the binding energies, one expects a slightly smaller

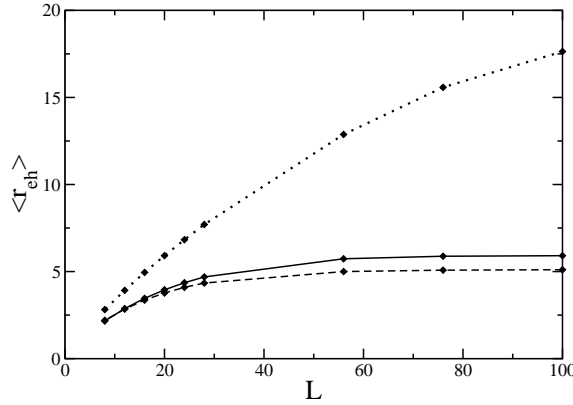


Figure 3. Average electron-hole distances $\langle r_{eh} \rangle$ from (10) as a function of system size L : dashed line **A**; solid line **B**; dotted line **C** (cf. table 1).

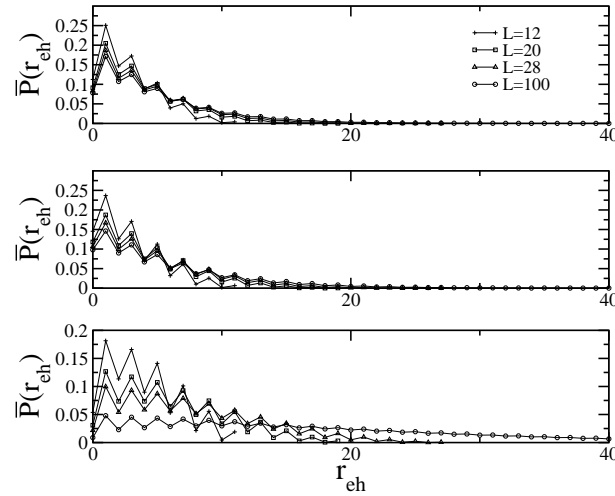


Figure 4. $\bar{P}(r_{eh})$ (9) for $L = 12, 20, 28, 100$: top panel **A**; middle panel **B**; bottom panel **C** (cf. table 1).

$\langle r_{eh} \rangle$, larger A , and smaller m_{qp} for the parameters **B** than for the set **A**, in contrast to what is seen. The reason for this behavior lies in the substantial difference in the Peierls dimerization Δ between both cases. Apparently, the Peierls dimerization Δ plays an important role for the structure of the excited-state wave function.

In figure 4 the probability function $\bar{P}(r_{eh})$, equation (9), is shown. A bound electron-hole pair leads to narrow probability distributions whose shape does not vary much with system size. An unbound pair leads to distributions which broaden with increasing system size, in accordance with the previous findings. The zigzag structure of $\bar{P}(r_{eh})$ can be explained by fluctuations in the ratio of double to single bonds at distance r_{eh} : Even distances r_{eh} cover always the same amount of single and double bonds, while odd distances can have one double bond more. As the electron-hole pairs form predominantly on double bonds, the value of $\bar{P}(r_{eh})$ fluctuates.

4.2. Excited-state wave function

Finally, the full probability function is addressed: $P(i, j)$ from equation (8). A bound electron-hole pair produces large values of $P(i, j)$ along the diagonal, where $i \approx j$. Accordingly, the off-diagonal region does not carry significant weight, because large distances between electron and hole are not probable.

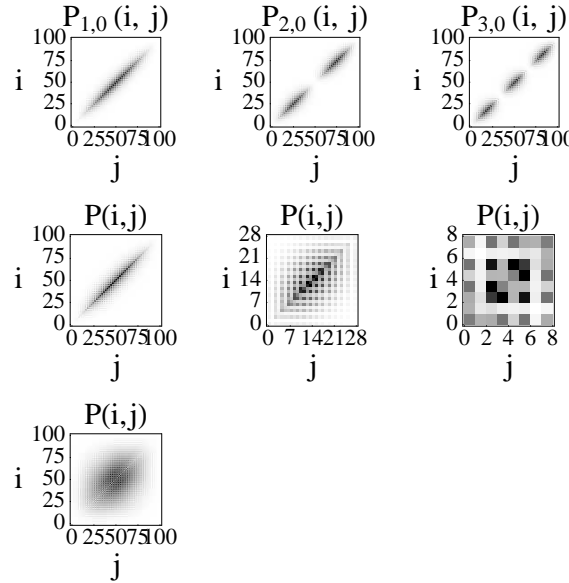


Figure 5. $P_{s,0}(i, j)$ from (8), parameter sets from table 1. Upper row: first three excited states (bound electron-hole pairs) using the parameter set **A** for $L = 100$; middle row: first excited states using the parameter set **B** for $L = 100, 28, 8$; bottom row: first excited state (unbound particle-hole pair) using the parameter set **C** for $L = 100$.

This plot also reveals whether or not the electron-hole pair is localized in a certain region of the oligoene. A continuous distribution of weight along the diagonal is a signature of a pair which is delocalized over the whole system which is to be expected for a perfectly ordered system.

The graphs of the first two rows of figure 5 are virtually identical for parameter sets **A** and **B**. Therefore, only parameter set **A** is used in the first row, where $P(i, j)$ is shown for the first, second, and third excited state and the size of the oligomer is fixed at $L = 100$. All three cases correspond to bound electron-hole pairs, and differ only in the number of nodes in their wave function. Apparently, the notion of a ‘electron-hole-pair-in-a-box’ very well applies to this case. The states with an even number of maxima in $P(i, j)$, i.e., the states with ‘gerade’ symmetry under inversion, carry no spectral weight in the optical absorption.

In the second row of figure 5 only systems from parameter set **B** are shown whose size is varied and only the first excited state is examined. On the left panel, for $L = 100$, a delocalized electron-hole pair is seen. In the middle panel, for $L = 28$, the oligomer

is large enough to support a bound electron-hole pair, and $P(i, j)$ quickly drops to zero in the off-diagonal region. For the smallest oligomer investigated, $L = 8$ on the right panel, the scattering by the boundaries is too strong to allow a bound pair.

In the third row of figure 5 the first excited state is displayed for the parameter set **C** and $L = 100$. In contrast to the first panels for the other two parameter sets, there is considerable weight in the non-diagonal parts of $P(i, j)$, a clear signature of an unbound electron-hole pair.

These considerations only apply to perfectly ordered oligomers. The next section shows, how disorder affects this picture.

5. Results for disordered chains

5.1. Disorder model

For the description of hard- and soft-disorder effects only the parameter set **A** is used. In order to incorporate soft-disorder effects in the microscopic description, it is assumed that the molecules do not have a planar, zig-zag geometric structure, but that the single bonds in the oligoenes are free to rotate. Due to the π -conjugation one expects an energy cost for the rotation of a single bond: the conjugation is broken, if the π orbitals are orthogonal to each other. One would therefore expect that a reasonable estimate for the torsion angles will not exceed $\vartheta \approx 40^\circ$. This is the most simple way to include disorder on a low-energy scale.

A disordered oligoene then consists of rotated single bonds along the chain with rotation angles ϑ taken at random from a chosen probability distribution. To lowest order one may assume that this rotation only affects the electron-transfer integral t_s for the $(L - 2)/2$ single bonds, which are substituted by a random number. For simplicity, the numbers t_s are taken with uniform probability from an interval which is set by $|t_s^{\min}| < |t_s^{\text{order}}| = 1 - \Delta/2$,

$$t_s \in [t_s^{\text{ord}}, t_s^{\min}] . \quad (16)$$

For fixed t_s^{\min} one averages over 20 realizations for every nominal oligomer length L .

By varying t_s^{\min} it is possible to adjust the disorder strength. A rough estimate of the relation between the electron-transfer integral and the rotation angle $t_s(\vartheta)$ can be inferred from the following argument. A rotation by $\vartheta = \pi/2$ reduces $|t_s|$ from the ordered values $|t_s^{\text{order}}|$ (parallel orbitals) to zero (orthogonal orbitals), and $t_s(\vartheta)$ should be symmetric and 2π -periodic. The choice

$$t_s(\vartheta) = t_s^{\text{ord}} \cos(\vartheta) . \quad (17)$$

fulfills these conditions. The maximal angle is obtained from $|t_s^{\min}| = |t_s(\vartheta_{\max})|$. Certainly, not all single bonds are affected by disorder in the same way, for example there can be correlations in the twisting angles from site to site. Nevertheless, this description of the soft disorder should be reasonable as long as ϑ_{\max} is not too large.

The disorder model (16) with small $|\vartheta_{\max}|$ in (17) lacks hard disorder due to kinks, chemical/physical impurities, and the like. Some of these sources of disorder act as a source of ‘soft disorder’ but they may also lead to a disruption of the oligomer chain. As in [18], ‘hard disorder’ for oligomers of nominal length L is defined via the statistical average over a uniform distribution of oligomer chains of the length $L_i \leq L$. All oligomer chains are also subject to the soft disorder model with $|t_s^{\min}| = 0.71$.

A very simplistic model for the probability distribution of the L_i is the assumption that the $L = 100, 76, 56$ oligomers can only break into shorter segments of length $L_1 = 28$, $L_2 = 56$, $L_3 = 76$. This means that a film of the $L = 100$ oligomer is assumed to consist of molecules of length 100, 76, 56, and 28 each having the same concentration. A film of the $L = 76$ oligomer consists of molecules of length 76, 56, and 28 with the same concentration. Finally, a film of the $L = 56$ oligomer consists of molecules with $L = 56$ and $L = 28$ in equal shares. A justification of this assumption is given in Sect. 5.3). This somewhat overestimates the importance of the longer chains as in [18] and makes the effects of hard disorder less prominent.

5.2. Soft disorder

5.2.1. Optical spectra In figure 6 the spectral weight $\overline{W}_L(E)$ of the first nine excited states for $L = 100$ is shown. This quantity is defined by the average over M disorder realizations with Gaussian broadening η ,

$$\overline{W}_L(E) = \frac{1}{M} \sum_{m=1}^M W_s^m(L) \mathcal{G}_\eta(E_s^m - E), \quad (18)$$

$$\mathcal{G}_\eta(\omega) = \frac{1}{\eta\sqrt{\pi}} \exp\left(-\omega^2/\eta^2\right), \quad (19)$$

where $W_s^m(L)$ is the weight of the s th resonance in the m th realization at a given system size L , see (5). In this case $M = 20$ and $\eta = 3 \cdot 10^{-3}$ which is of the order of the maximum DMRG error η_a .

As seen in the left part of figure 6 not much changes for small twisting angles. When $\vartheta_{\max} = 12^\circ$, the individual resonances keep their relative weight and they are clearly resolved. Thus, the behavior very much resembles the ordered case, see figure 1.

In the right part of figure 6, where $\vartheta_{\max} = 28^\circ$, the influence of the disorder is much more pronounced. Substantial spectral weight is shifted from the first to the second resonance which, due to the presence of disorder, is no longer symmetry-forbidden. The line spectrum is considerably smeared out, but individual resonances are still discernible, and the spectrum is shifted to higher energies. Nevertheless, the distribution of single-particle gaps is still small enough to identify a binding energy of the electron-hole pair of the order of $0.1t$ (see error bar in figure 6).

A further increase of the disorder ($|t_s^{\min}| = 0.4$, $\vartheta_{\max} = 60^\circ$) leads to the situation where different resonances from different realizations contribute to the same frequency, and individual lines can no longer be identified. Finally, for very strong disorder fluctuations ($|t_s^{\min}| = 0$, $\vartheta_{\max} = 90^\circ$), the inhomogeneous width of the first excited

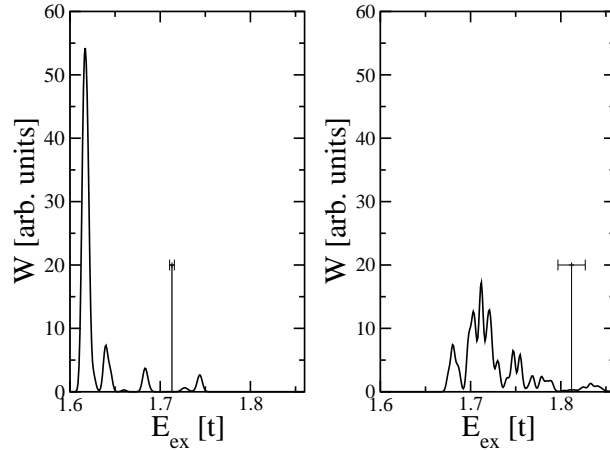


Figure 6. Spectral weight $\overline{W}_L(E)$ of the first nine excited states for $L = 100$ and the parameter set **A** (table 1), averaged over 20 realizations. Left: $|t_s^{\min}| = 0.79$ ($\vartheta_{\max} = 12^\circ$); right: $|t_s^{\min}| = 0.71$ ($\vartheta_{\max} = 28^\circ$). A thin vertical line marks the one-particle gap of equation (11) with its standard deviation added on top.

state is of the same order as its binding energy. Both situations are not supported by experiments [2]. Therefore, $t_s^{\min} = 0.71$, i.e., moderate twisting angles of $\vartheta \leq 28^\circ$, should be taken as reasonable values for the (soft) disorder model and the parameter set **A**. This is also an a posteriori justification of the chosen disorder model, as one does not need unrealistically large values of ϑ_{\max} in order to describe the experimentally observed disorder effects.

5.2.2. Binding energy and distance of the electron-hole pair As seen from figure 7 the shift to higher excitation energies with increasing disorder occurs for all oligomer sizes. Also shown in the figure are the average excitation energy of the lowest excitation $\overline{E}_{\text{ex}}(L)$ and the average one-particle gap $\overline{E}_{\text{gap}}(L)$. The bars on the data points indicate the standard deviations $\delta E_{\text{ex}}(L)$ and $\delta E_{\text{gap}}(L)$ for the configuration average,

$$\begin{aligned} \overline{E}_{\text{ex}}(L) &= \frac{1}{M} \sum_{m=1}^M E_{\text{ex}}^m(L) , \\ \overline{E}_{\text{gap}}(L) &= \frac{1}{M} \sum_{m=1}^M E_{\text{gap}}^m(L) , \end{aligned} \quad (20)$$

$$(\delta E_{\text{ex}}(L))^2 = \frac{1}{M} \sum_{m=1}^M [E_{\text{ex}}^m(L) - \overline{E}_{\text{ex}}(L)]^2 , \quad (21)$$

$$(\delta E_{\text{gap}}(L))^2 = \frac{1}{M} \sum_{m=1}^M [E_{\text{gap}}^m(L) - \overline{E}_{\text{gap}}(L)]^2 ,$$

and averages of other quantities are obtained accordingly. $\delta E_{\text{ex}}(L)$ increases from the order of 10^{-3} to the order of 10^{-2} when the disorder is increased from $|t_s^{\min}| = 0.79$ to $|t_s^{\min}| = 0.71$ which is the reason for the observed inhomogeneous line broadening in figure 6.

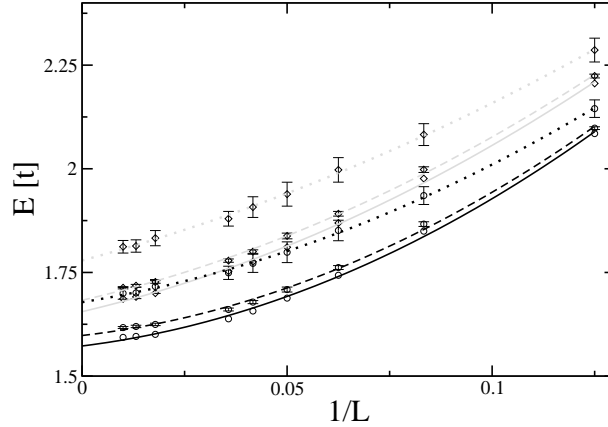


Figure 7. Average excitation energy $\overline{E}_{\text{ex}}(L)$ (circles) and average one-particle gap $\overline{E}_{\text{gap}}(L)$ (diamonds), see (20), for oligoenes with $8 \leq L \leq 100$ in the Peierls-Hubbard model (3) for the parameter set **A** (table 1). All lines are quadratic fits to the data presented. Solid lines: ordered case $|t_s^{\min}| = |t_s^{\text{ord}}| = 0.81$; dashed lines: $|t_s^{\min}| = 0.79$ ($\vartheta_{\max} = 12^\circ$); dotted lines: $|t_s^{\min}| = 0.71$ ($\vartheta_{\max} = 28^\circ$). The inhomogeneous broadening is indicated by the standard deviations (21); they are discernible only for $|t_s^{\min}| = 0.71$.

The quadratic dependence of the average gap and excitation energy with respect to the inverse oligomer size $1/L$ is preserved. However, the lines in figure 7 are not described by (13) anymore, but by functions with an additional linear term in $1/L$. This is in qualitative agreement with the analysis of Ref. [19] which lead to (2). For a quantitative analysis, larger system sizes and more realizations are required; this is beyond the scope of the present work.

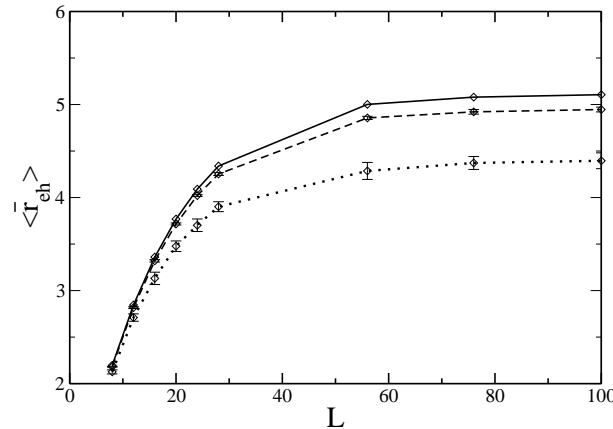


Figure 8. Average electron-hole distance, $\overline{\langle r_{\text{eh}} \rangle}$ from (10), as a function of L and the parameter set **A** (table 1). Solid lines: ordered case, $|t_s^{\min}| = |t_s^{\text{ord}}| = 0.81$; dashed lines, $|t_s^{\min}| = 0.79$ ($\vartheta_{\max} = 12^\circ$); dotted lines, $|t_s^{\min}| = 0.71$ ($\vartheta_{\max} = 28^\circ$).

The overall offset of the average energies requires a closer inspection of the excited-state wave function. In figure 8 the average electron-hole distance is shown, $\overline{\langle r_{\text{eh}} \rangle}$ from

equation (10), as a function of L . For the parameters chosen one still finds a bound electron-hole pair which, at the same L , appears to be slightly *smaller* and more tightly bound than the electron-hole pair in the ordered system.

5.2.3. Excited-state wave function The full distribution function $P^m(i, j)$ for realizations m of the disorder, as shown in figure 9, reveals an additional effect of disorder: localization. All cases show that there is substantial weight only on the diagonal, which is the signature of bound electron-hole pairs. The disorder effect on $P(i, j)$ is twofold: the distribution is distorted, as shown on the right part of figure 9, and it is ‘localized’ in the sense that there are substantial parts on the diagonal where $P^m(i, i) \ll \text{Max}\{P^m(i, i)\}$, see the left part of figure 9. With increasing disorder, the fraction of oligomers that show a single-segment localization increases. For $|t_s^{\min}| = 0.71$ ($\vartheta_{\max} = 28^\circ$), 18 of 20 oligomers give rise to a single-segment $P(i, j)$. In any case, one expects that the disorder localizes the electron-hole pair because single-particle wave functions are generically localized in one dimension [27]. It is important to note that the segments are formed even though this is not an inherent property of the used disorder model. The segments are formed by the underlying fluctuation of the t_s : the fluctuations are comparatively small over the range of the segment, and its boundaries are determined by sudden drops in t_s .

As the electron-hole pairs are constrained to chain segments, one can define a length scale set by the disorder, r_{seg}^m , which represents the number of carbon atoms on which the electron-hole pair is present. As a cut-off criterion $P^m(i, i) > 10^{-5} \approx 10^{-2}\text{Max}_i\{P(i, i)\}$ is chosen, i.e., one demands the probability to be at least one percent of the peak probability for the ordered case. From this the average length of the segments as in (21) is calculated.

Table 3. Average binding energy \overline{E}_b , average electron-hole distance $\overline{\langle r_{\text{eh}} \rangle}$, and average segment length $\overline{r}_{\text{seg}}$ for $L = 100$ of the first excited state in the EPH for the parameter set **A** (table 1). Standard deviations are given in square brackets as the uncertainty in the last given digit.

Disorder	\overline{E}_b	$\overline{\langle r_{\text{eh}} \rangle}$	$\overline{r}_{\text{seg}}$
none	0.092[0]	5.10[0]	81
$ t_s^{\min} = 0.79$	0.095[2]	4.94[2]	72
$ t_s^{\min} = 0.71$	0.11[1]	4.39[8]	47

The results are summarized in table 3 where the binding energy \overline{E}_b is given, the average electron-hole distance $\overline{\langle r_{\text{eh}} \rangle}$, and the average segment length $\overline{r}_{\text{seg}}$ for $L = 100$ in the EPH for the parameter set **A**. As mentioned above, the average electron-hole distance decreases for increasing disorder strength. The reason for this decrease is not the increase of the binding energy, a quantity which not only depends on the energy of the excited-state resonance but also on the size of the single-particle gap. Instead, the disorder ‘squeezes’ the electron-hole pairs into segments of length $\overline{r}_{\text{seg}}$. In the clean

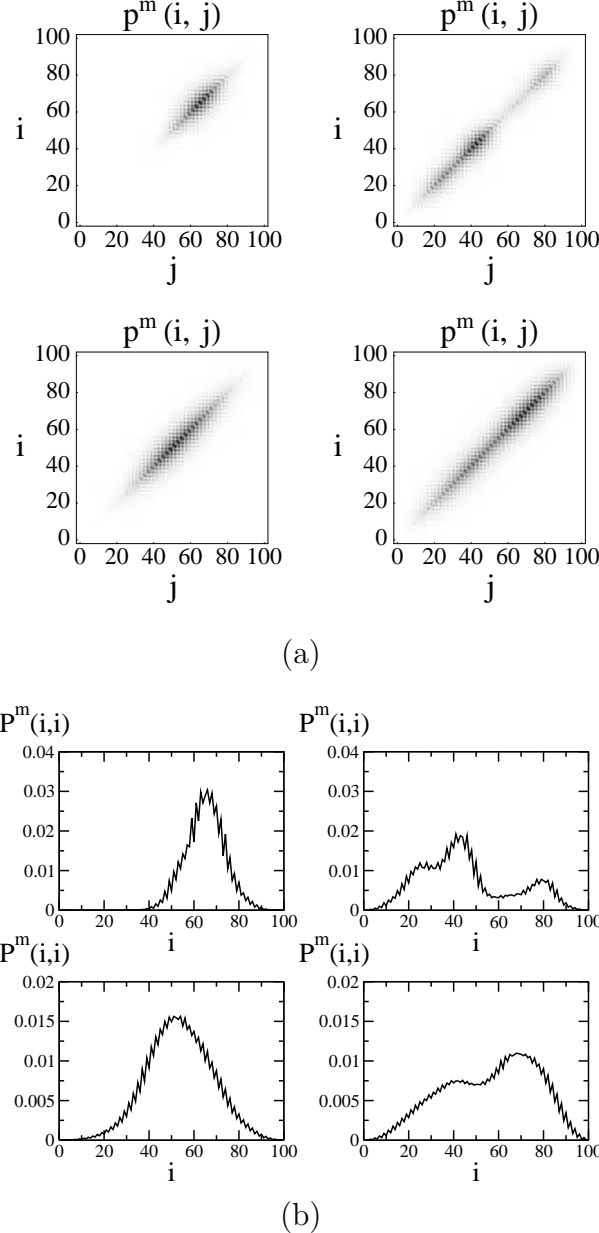


Figure 9. (a) Excited-state wave functions $P^m(i, j)$ (8) for two different realizations for $L = 100$ and the parameter set \mathbf{A} (table 1). Upper row: $|t_s^{\min}| = 0.71$ ($\vartheta_{\max} = 28^\circ$), lower row: $|t_s^{\min}| = 0.79$ ($\vartheta_{\max} = 12^\circ$). Left part: single-domain localization, right part: multiple-domain localization: (b) $P^m(i, i)$ cut along the diagonal from (a), $P^m(i, i)$.

system, the excited-state wave function essentially spreads over the whole chain, and one sees a reduction only at the chain ends. In contrast, in the presence of substantial disorder the electron-hole pair is squeezed into regions which are much smaller than the nominal oligomer size. For example, for $L = 100$ and $\vartheta_{\max} = 28^\circ$ the system almost acts as if it was an ordered chain about half the actual size, with a concomitant reduction of the electron-hole distance and an increase of the binding energy, compare figure 7.

A close inspection of the excitation energies shows that ordered chains of the same size as the segments have smaller excitation energies. The smaller chains show the same excitation energy, however, if they exhibit the same fluctuation of the t_s as in the segment. The conclusion is that a long oligomer can be described by a small, disordered segment.

5.3. Hard disorder

The model for soft disorder must be supplemented by a model for hard disorder in order to include the effects of kinks and impurities (see Sect. 5.1). Figure 10 shows the result of the averaging procedure for the optical spectra. When an oligomer of nominal length $L = 100$ is investigated and it is broken into pieces of length $L_i = 28, 56, 76, 100$, then the first excitation broadens and higher excitations have a very small weight (upper left panel in figure 10). One can make the same observation for $L = 76$ ($L_i = 28, 56, 76$) and for $L = 56$ ($L_i = 28, 56$). In addition, those spectra resemble closely the one for $L = 100$, which is a signature of the expected saturation effect [18]. Only small chains, $L = 28$, where only soft disorder is present, permit the clear identification of isolated and narrow excited-state resonances.

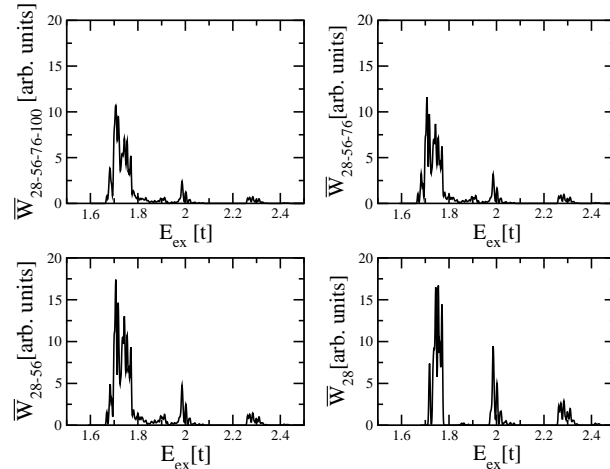


Figure 10. \bar{W}_L as in figure 6 for the parameter set **A** (table 1) and $|t_s^{min}| = 0.71$. From left to right the arithmetic average is displayed over the results for 20 realizations for soft disorder at lengths $L = 100$ ($L_i = 28, 56, 76, 100$), $L = 76$ ($L_i = 28, 56, 76$), $L = 56$ ($L_i = 28, 56$), and $L = L_i = 28$.

Given the width of the structures it becomes difficult to assign a unique energy to the excitation. Therefore, the center of gravity of the distributions for the first excitation in figure 10 is taken as representative for the position of the ‘typical’ resonance $E_{ex}^{hd}(L)$ with $L = 100, 76, 56$. These three energies as a function of nominal system size L are shown in figure 11 (dotted line), together with the excitation energy of the ordered systems and the soft-disorder model. As expected, the energy of the ‘typical’ excitation shifts further upwards with respect to the soft-disorder case and one observes the typical

saturation effect. Even though the effects of the longest chains have been overestimated, $E_{\text{ex}}^{\text{hd}}(L)$ saturates quickly close the excitation energy for the shortest, unbroken chain $E_{\text{ex}}(L = 28)$ as predicted by [18].

6. Summary

In this work it has been confirmed that the generic size-dependence of the excitation energy of the first optically allowed state for large, ordered oligoenes is purely quadratic in $1/L$ [13, 14]. This behavior is most easily understood for the case of bound electron-hole pairs which can be described as independent particles in a box. Thus the electron-electron interaction indeed introduces a new length scale, the electron-hole distance, $\langle r_{\text{eh}} \rangle$, which one can easily deduce from the wave-function analysis. However, the generic scaling can only be seen when the system size is considerably larger than the electron-hole distance and the system is ordered.

‘Medium-sized’, ordered oligomers of the order of several electron-hole distances show substantial deviations from the quadratic law. In this region, a linear fit in $1/L$ better describes the data for the excitation energy. However, this is accidental for ordered oligomers and mostly due to the applicability of Taylor’s theorem to smooth functions. In fact, a regular behavior cannot be expected because two effects, binding and scattering of the pair by the boundaries, compete with each other for medium system sizes. This is even more the case for the smallest oligomers.

Soft disorder, e.g., fluctuations in the bending angle between neighboring carbon atoms on single bonds, sets a length scale \bar{r}_{seg} on which electron-hole pairs are localized. This localization leads to a hypsochromic shift in the excitation energies. One can also observe a redistribution of spectral weight due to symmetry breaking, and inhomogeneous broadening of spectral lines, as expected. Additionally, the dependence

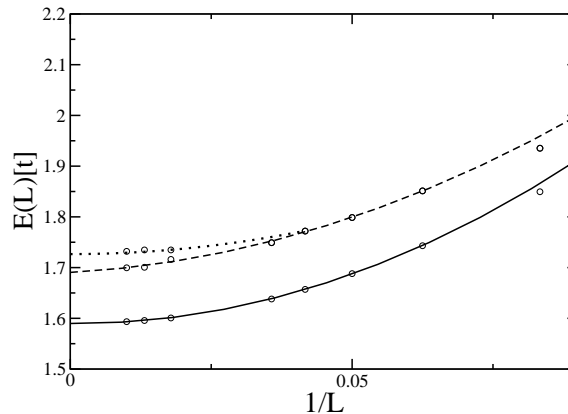


Figure 11. Excitation energies of parameter set **A** (table 1). solid line: ordered oligomers (figure 2); dashed line: soft-disorder model with $|t_s^{\text{min}}| = 0.71$; dotted line: hard-disorder model with $|t_s^{\text{min}}| = 0.71$ and arithmetic averaging over oligomer chains (figure 6).

of the excitation energies on $1/L$ clearly shows a linear term.

The length scale \bar{r}_{seg} slowly increases with nominal system size L . However, it is difficult to observe experimentally oligomers with the full nominal size. Instead, on top of the soft disorder, there are kinks and impurities which effectively cut a long oligomer into segments of a typical size L_{typ} so that oligomers of a typical length with a typical \bar{r}_{seg} dominate the optical excitation spectrum. The chance to observe well-ordered long segments very slowly increases as a function of nominal chain length L .

In this work an interpretation scheme has been used for the excited-state wave functions which has been developed earlier [21]. This scheme is seen to work equally for ordered as well as disordered systems, for semi-empirical methods as well as for EPH. Moreover, the results indicate that the models for soft and hard disorder provide a suitable description of disorder in π -conjugated oligomers. This work did not aim at a quantitative description of the optical absorption of polymer films. For example, experimental data [28] suggest a much steeper descend of $E_{\text{ex}}(L)$ from $L = 8$ to $L = 16$ than can be described using the parameter sets **A**, **B**, and **C**. Additionally, the electron-hole distance $\langle r_{\text{eh}} \rangle$ which is experimentally available via electro-absorption [4], is not perfectly reproduced even though it is found to be of the right order of magnitude. An improved description for ordered polydiacetylenes, e.g., with long-range interactions and polaronic relaxations, should remedy these shortcomings.

Acknowledgments

This work was funded by the Deutsche Forschungsgemeinschaft under GE 746/7-1. J.R. gratefully acknowledges support by the Alexander von Humboldt Stiftung. This work was supported in part by the center *Optodynamik* of the Philipps-Universität Marburg.

References

- [1] Brédas J-L and Silbey R (ed) 1991 *Conjugated Polymers* (Dordrecht: Kluwer, Dordrecht) *Conjugated Polymers and related Materials*, ed. by W.R. Salaneck, I. Lundström (Oxford University Press, Oxford, 1993).
- [2] Wegner G and Müllen K (ed) 1996 *Electronic Materials: The Oligomer Approach*, ed. by (Weinheim: Wiley-VCH)
- [3] Meier H, Stalmach U and Kolshorn H 1997 *Acta Polymer.* **48** 379
- [4] Sebastian L and Weiser G 1981 *Phys. Rev. Lett.* **46** 1156
Weiser G 1992 *Phys. Rev. B* **45** 14076
Horvath A, Weiser G, Lapersonne-Meyer C, Schott M and Spagnoli S 1996 *Phys. Rev. B* **53** 13507
Harrison M G, Möller S, Weiser G, Urbasch G, Mahrt R F, Bäßler H and Scherf U 1999 *Phys. Rev. B* **60**, 8650
- [5] See, for example, Heeger A J, Kivelson S, Schrieffer J R and Su W-P 1988 *Rev. Mod. Phys.* **60** 781
- [6] Ovchinnikov A A, Ukrainskii I I and Kvetsel G V 1972 *Usp. Fiz. Nauk* **108** 81 [1973 *Sov. Phys.-Usp.* **15** 575].

- [7] For a review, see Baeriswyl D, Campbell D K and Mazumdar S 1992 *Conjugated Conducting Polymers Springer, Series in Solid State Sciences* vol 102 ed H. Kiess (Berlin: Springer) p 3
- [8] See, for example, Greene B I, Orenstein J, Millard R R and Williams L R 1987 *Phys. Rev. Lett.* **58** 2750
Abe S, Yu J and Su W-P 1992 *Phys. Rev. B* **45** 8264.
- [9] Rohlfing M and Louie S G 1999 *Phys. Rev. Lett.* **82** 1959
- [10] van der Horst J W, Bobbert P A, Michels M A J, Brocks G and Kelly P J 1999 *Phys. Rev. Lett.* **83** 4413
van der Horst J W, Bobbert P A, de Jong P H L, Michels M A J, Brocks G and Kelly P J 2000 *Phys. Rev. B* **61** 15817
- [11] Gebhard F, Bott K, Scheidler M, Thomas P and Koch S W 1997 *Phil. Mag.* **75** 1
——— 1997 *Phil. Mag.* **75** 13
——— 1997 *Phil. Mag.* **75** 47
- [12] Pleutin S and Fave J L 1998 *J. Phys. Cond. Matt.* **10** 3941
- [13] Boman M and Bursill R J 1998 *Phys. Rev. B* **57** 15167
- [14] Jeckelmann E 1998 *Phys. Rev. B* **57** 11838
- [15] Barford W, Bursill R J and Lavrentiev M Y, 2001 *Phys. Rev. B* **63** 195108
- [16] Ramasesha S, Pati S K, Shuai Z and Brédas J-L 2001 *Adv. Quantum Chem.* **38** 121
- [17] Race A, Barford W and Bursill R J 2003 *Phys. Rev. B* **67** 245202
- [18] Kohler B E and Woehl J C 1995 *J. Chem. Phys.* **103** 6253
- [19] Rossi G, Chance R R and Silbey R 1990 *J. Chem. Phys.* **90** 7594
- [20] White S R 1992 *Phys. Rev. Lett.* **69** 2863
——— 1993 *Phys. Rev. B* **48** 10345
- [21] Rissler J, Bäßler H, Gebhard F and Schwerdtfeger P 2001 *Phys. Rev. B* **64** 045122
- [22] Peschel I, Wang X, Kaulke M and Halberg K (ed) 1999 *Density-Matrix Renormalization Group, A New Numerical Method in Physics, Lecture Notes in Physics* vol 258 (Berlin: Springer)
- [23] Jeckelmann E 2002 *Phys. Rev. B* **66** 045114
- [24] Woynarovich F 1982 *J. Phys. C* **15** 85
- [25] Essler F H L, Göhmann F, Frahm H, Klümper A and Korepin V 2004 *The One-Dimensional Hubbard Model* (Cambridge: Cambridge University Press)
- [26] Lou J, Qin S, Ng T-K, Z. Su and I. Affleck 2000 *Phys. Rev. B* **62** 3786
- [27] Mott N F and Twose W D 1961 *Adv. Phys.* **10**, 107Borland R E 1963 *Proc. Roy. Soc. London Ser. A* **274** 529Landauer R 1970 *Phil. Mag.* **21** 863Thouless D J 1977 *Phys. Rev. Lett.* **39** 1167
- [28] Kohler B E 1990 *J. Chem. Phys.* **93** 5838